Inorganic Chemistry

Communication

pubs.acs.org/IC

Monoclinic $Ag_2Mo_2O_7$ Nanowire: A New Ag−Mo−O Nanophotocatalyst Material

Kenji Saito,*[†,‡] Shotaro Kazama,[†] Kazuki Matsubara,[†] Tatsuto Yui,[†] and Masayuki Yagi[†,‡]

[†]Department of Materials Science and Technology, Faculty of Engineering, Niigata University, 8050 Ikarashi-2, Niigata 950-2181, Japan

[‡]PRESTO, Japan Science and Technology Agency, 4-1-8 Honcho, Kawaguchi, Saitama 332-0012, Japan

Supporting Information

ABSTRACT: We report a template-free facile technique that allows for the first ever synthesis of a *monoclinic* $Ag_2Mo_2O_7$ nanowire (m-$Ag_2Mo_2O_7$-NW), using a commercially available MoO_3 particle. The nanowire possessed high crystallinity and structural homogeneity and strongly suggested that the nanowire was grown through an oriented aggregation mechanism in contrast to the case of a typical solution-phase method. The corresponding bulky counterpart showed no photoresponse; however, a complete structural transformation toward a nanowire triggered activity for O_2 evolution in the presence of Ag^+ as an electron acceptor under visible-light irradiation.

Solar-to-fuel conversion using a photocatalyst has merited special attention as one of the promising ways to overcome recent energy issues caused by the existing energy systems being dependent largely on fossil fuels. A potential candidate for use as the photocatalyst includes a semiconductor nanowire. Actually, visible-light-responsive photoelectrocatalysts made up of the nanowires have been reported to show enhanced performance in comparison to the corresponding bulky counterparts.[1−7] The enhanced performance is involved in the low radial dimension and high surface-to-volume ratio, both of which facilitate charge separation due to the small distance of photogenerated carrier transfer from bulk to surface and anisotropic carrier transport along the growth direction of a one-dimensional (1D) nanowire.[1−7] So far, there have been only a few reports regarding heterogeneous nanowire photocatalysts with visible-light response, i.e., CdS, $BiVO_4$, GaP, GaN, and $NaNbO_3$−$AgNbO_3$ core−shell structure.[8−12] However, most nanowires showed poor phocatalytic activities in comparison to the corresponding bulky counterparts. Although a hydrothermal synthesis,[8,9] a solution−liquid−solution method,[10] and a metal-complex-based synthesis[11] have so far been known as large-scale preparation methods for the nanowires, a simpler and more elegant way to fabricate the nanowire possessing superior functionality is highly desired.

We report herein the first ever synthesis of an m-$Ag_2Mo_2O_7$ (Figure S1 in the Supporting Information, SI) nanowire (m-$Ag_2Mo_2O_7$-NW) by a quite simple strategy and observation of the photocatalytic O_2 evolution r under visible-light irradiation.

X-ray diffraction (XRD) patterns of powder obtained after reflux of an aqueous $AgNO_3$ suspension containing commercially available MoO_3 for 5 h were different from those of MoO_3 and were indexed with m-$Ag_2Mo_2O_7$ with unit cell parameters: a = 6.1138(5) Å, b = 13.1641(12) Å, and c = 7.8730(4) Å (Figure S2 in the SI). Field-emission scanning electron microscopy (FE-SEM) image of the powder showed only nanowire morphology with ca. 200 nm diameter (Figure S3a in the SI). This geometry was in sharp contrast to that of the MoO_3 particles (Figure S3b in the SI). High-resolution transmission electron microscopy (HR-TEM) measurements were conducted in order to gain more insight into the crystal structure and sample purity of m-$Ag_2Mo_2O_7$-NW (Figure S4 in the SI). Nanoparticles exhibiting dark contrasts were seen throughout the nanowire surface. A fast Fourier transformation (FFT) image (Figure S5 in the SI) taken from the HR-TEM image agreed well with that of *cubic* Ag (PDF 4-783). In addition to the Ag nanoparticles, a 7-nm-thick layer composed of amorphous molybdenum oxide (MoO_x), as revealed by elemental analyses shown in Table S1 in the SI, existed on the nanowire surface (Figure S4a in the SI). X-ray photoelectron spectroscopy (XPS) analysis of m-$Ag_2Mo_2O_7$-NW before the TEM measurement represented the absence of a metallic Ag component (Figure S6 in the SI). Considering that, after the high-resolution observation accompanied with light focus, the MoO_x layer was undetectable on the opposite sidewall being not focused (Figure S4c in the SI), the light focus led to the promotion of partial decomposition of $Ag_2Mo_2O_7$ to afford the MoO_x layer coupled with Ag nanoparticles. The electron-beam disruption of Ag-containing metal oxide is sometimes seen, as is the case for $Ag_2Mo_3O_{10}\cdot 1.8H_2O$.[13] HR-TEM images revealed clear lattice fringes, and the widths of the fringes were determined to be 1.31 ± 0.03 nm. The value agrees well with the d spacing of (010) of m-$Ag_2Mo_2O_7$ (d_{010} = 1.31 nm). As shown in Figure S4b in the SI, an inverse FFT image taken from Fourier components of Figure S4a in the SI highlighted a highly crystalline surface. Nano electron diffraction provided further confirmation of the single-crystalline nature of the nanowire (Figure 1a). In addition, [−201] perpendicular to [010] indicated the growth direction of m-$Ag_2Mo_2O_7$-NW. Figure S1c in the SI displays the crystal structure of m-$Ag_2Mo_2O_7$ along [−201], indicating that 1D growth occurs in a direction along edge- and corner-shared MoO_6 units and three-dimensionality is created by lateral growth involving interchain connections. Elemental analysis of the single nanowire was conducted as well (Table S1 in the SI). The mole ratio of Ag to Mo was 1.10 ± 0.08, which corresponded to $Ag_2Mo_2O_7$. The nanowire was found to

Received: May 16, 2013
Published: July 17, 2013

   dx.doi.org/10.1021/ic401236b | *Inorg. Chem.* 2013, 52, 8297−8299

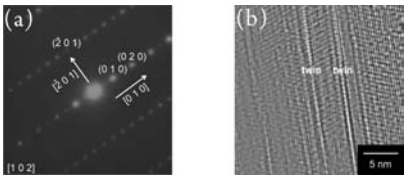

Figure 1. (a) Nano electron diffraction and (b) images displaying discrete twin domains included in the m-$Ag_2Mo_2O_7$-NW sample.

possess an exceptionally low Brunauer−Emmett−Teller (BET) surface area (2 m^2 g^{-1}), whereas semiconductor nanowires possessed 50−200 m^2 g^{-1} in general.[8−11] This may originate from a very smooth nanowire surface, as recognized by HR-TEM images (Figure S4a,b in the SI).

A growth mechanism of the nanowire crystal includes the following three possibilities: (1) single-crystal growth reflecting the crystal structure of m-$Ag_2Mo_2O_7$, which possesses an asymmetric 1D chain structure (Figure S1 in the SI), (2) coarsening (Ostwald ripening).[14−18] The first one is quite unlikely because vigorous stirring conditions basically prevent single-crystal growth (see the experimental section). The other possibilities (2 and 3) are known to be mechanisms of template-free nanocrystal growth.[16−18] To distinguish these, several control experiments were carried out. The reflux experiments being terminated just 5 min later gave nanowires with very small diameters on the MoO_3 particles besides already formed nanowires, as shown in Figure S7 in the SI. The existence of the small-diameter nanowires suggests a side-by-side self-assembly process[18] and cannot be accounted for by Ostwald ripening. In addition, the final form of the $Ag_2Mo_2O_7$ nanowire (after 5 h of reflux) contained a twin structure of $Ag_2Mo_2O_7$, as evidenced by the HR-TEM image (Figure 1b). These results strongly suggest that m-$Ag_2Mo_2O_7$-NW is formed through the oriented aggregation mechanism.[16−18] Here, a m-$Ag_2Mo_2O_7$ *microrod* has so far been prepared by a hydrothermal method using $(NH_4)_6Mo_7O_{24}{\cdot}4H_2O$ and $AgNO_3$.[19] To confirm the influence of reflux under ordinary pressure and the starting materials on the structure and growth mechanism of $Ag_2Mo_2O_7$, we first examined 5 h of reflux of an aqueous $AgNO_3$ suspension containing $(NH_4)_6Mo_7O_{24}{\cdot}4H_2O$ as the Mo source. The powder obtained showed XRD patterns characteristic of m-$Ag_2Mo_2O_7$ and possessed a slightly small-diameter microrod structure; however, less structural homogeneity was the same as that in the previous work (Figure S8a in the SI).[19] In addition, after termination of the reaction for 5 min, a small-diameter nanowire was not detected in the sample (Figure S8b in the SI). Thus, formation of the nanoparticles in the initial stage of $Ag_2Mo_2O_7$ synthesis suggested an Ostwald ripening mechanism. The reason why the different growth mechanisms occur by just a change in the starting materials involves in the solubility. Solubilities in water of $(NH_4)_6Mo_7O_{24}{\cdot}4H_2O$, $AgNO_3$, and MoO_3 are 0.30 g mL^{-1} (298 K), 2.19 g mL^{-1} (293 K), and 0.49 mg mL^{-1} (301 K). The addition of water to $(NH_4)_6Mo_7O_{24}{\cdot}4H_2O$ and $AgNO_3$ crystals resulted in a suspension at room temperature. Fast nucleation generally occurs in the solution-phase method.[18] The primary particles will have a large size distribution, leading to crystal growth via a typical Ostwald ripening mechanism. By contrast, MoO_3 has much lower solubility in water than $(NH_4)_6Mo_7O_{24}{\cdot}4H_2O$; thereby a very slow supply of Mo ions to the solution medium by diffusion occurs throughout the MoO_3 microparticle to afford primary particles with a small size distribution on MoO_3. The end-to-end self-assembly of the primary particles or anisotropic crystal growth depending on their crystal planes exposed on the particles, to reduce the surface energy, promotes 1D growth. The small-diameter nanowires grown through the same mechanism align side-by-side to form a nanowire bundle and finally a single crystal (Scheme S1 in the SI). Assembly of the small-diameter nanowires was reported to occur even in the diameters ranging from 10 to 30 nm.[18] Our result seen in Figure S7 in the SI seems to be within the range. If the mechanistic hypothesis is correct, the final form of the nanowire structure should not be dependent on the morphology of MoO_3. Actually, when a MoO_3 microrod was used as the starting material, m-$Ag_2Mo_2O_7$ with the same homogeneous nanowire structure as m-$Ag_2Mo_2O_7$−NW given by MoO_3 was obtained, as shown in Figure S9 in the SI.

Figure S10 in the SI shows diffuse-reflectance spectrometry (DRS) spectra. The band gap of m-$Ag_2Mo_2O_7$-NW was estimated by the sharp absorption edge as 2.98 eV (416 nm). Then we screened the dimolybdate compounds, which will cause only an O^{2-} to Mo^{6+} transition, being worthy of the potential reference. Among the dimolybdate compounds,[20] MoO_6 octahedra running along the chain direction were only seen in $Na_2Mo_2O_7$ and $Cs_2Mo_2O_7$, and the others were formed from MoO_4 mixing with MoO_6 or an isolated MoO_4 unit. Thus, we selected $Na_2Mo_2O_7$ (3.25 eV) as the reference compound. Incorporation of Ag^+ into molybdenum oxide caused a gap narrowing of 0.27 eV. The reason for the narrowing will be attributable to contribution of the Ag 4d orbital to a hybrid orbital with O 2p as a valence band at a more negative potential than O 2p.

As shown in Figure S11 in the SI, m-$Ag_2Mo_2O_7$-NW showed the activity for the O_2 evolution reaction in the presence of $AgNO_3$ as an electron acceptor (0.8 V vs NHE). The O_2 evolution reaction did not proceed without $AgNO_3$ under identical reaction conditions. After the photocatalytic experiment, XRD and SEM measurements were conducted in order to check the compositional and structural changes of the nanowire, respectively. A slight amount of the Ag_2MoO_4 component was detected, as shown in Figure S12 in the SI, whereas the morphology of the nanowire was maintained during photoirradiation. The formation mechanism of Ag_2MoO_4 to be expected includes decomposition of $Ag_2Mo_2O_7$ into Ag_2MoO_4 and MoO_3 as follows:

$$Ag_2Mo_2O_7 \rightarrow Ag_2MoO_4 + MoO_3 \quad (1)$$

Using a mixed powder of Ag_2MoO_4 with an equimolar amount of MoO_3, the ratio of XRD peak intensities of the most intensive (311) due to Ag_2MoO_4 relative to (110) due to MoO_3, which is not overlapped with any Ag_2MoO_4 mirror indices, was confirmed to be 11; however, the MoO_3 component was not detected as the value to be expected (Figure S12 in the SI). Therefore, Ag_2MoO_4 should be formed by the reaction of $Ag_2Mo_2O_7$ with Ag^+ and H_2O as an oxygen source:

$$Ag_2Mo_2O_7 + 2AgNO_3 + H_2O \rightarrow 2Ag_2MoO_4 + 2HNO_3 \quad (2)$$

Ag_2MoO_4 detected by XRD as a byproduct showed no photoresponse at identical reaction conditions. In addition, the photocatalytic experiements using m-$Ag_2Mo_2O_7$-NW resulted in no induction period (Figure S11 in the SI). Thus, m-$Ag_2Mo_2O_7$-NW was found to have an intrinsic performance for the O_2 evolution reaction. Estimation of the photocatalytic activity for O_2 evolution over MoO_3 from an aqueous $AgNO_3$ solution under UV light (λ > 300 nm) was hampered because of in situ

dx.doi.org/10.1021/ic401236b | *Inorg. Chem.* 2013, 52, 8297−8299

formation of m-$Ag_2Mo_2O_7$-NW. The m-$Ag_2Mo_2O_7$ microrod (Figure S8 in the SI), which can be regarded as the bulk, showed no photoresponse. Thus, a complete structural transformation toward nanowire triggered photocatalytic activity. As shown in Figure S13 in the SI, the low-aspect-ratio $Ag_2Mo_2O_7$ nanoparticle (m-$Ag_2Mo_2O_7$-NP) prepared by just batch grinding of m-$Ag_2Mo_2O_7$-NW maintained its crystal structure, crystallinity [the full-widths at half-maximum for (200) peaks were 0.25° for m-$Ag_2Mo_2O_7$-NW and 0.26° for m-$Ag_2Mo_2O_7$-NP, respectively], and absorption feature (Figure S10 in the SI) and possessed a BET surface area (3 $m^2\ g^{-1}$) similar to that of m-$Ag_2Mo_2O_7$-NW (2 $m^2\ g^{-1}$). Nevertheless, m-$Ag_2Mo_2O_7$-NP showed a lower photocatalytic activity for the O_2 evolution reaction compared with m-$Ag_2Mo_2O_7$-NW (Figure S11 in the SI). This will be originated from the possibilities that crystal planes mechanically produced on the short axis of the nanowire are inactive for oxidation of water into O_2 or an anisotropic carrier-transport phenomenon to facilitate charge separation following visible-light irradiation require a distance of the long axis to some extent. Loading of a IrO_2 cocatalyst onto m-$Ag_2Mo_2O_7$-NW enhanced the photocatalytic performance (Figure S11 in the SI).[21] Long-term photoirradiation for 30 h did not afford additional Ag_2MoO_4 formation (eq 2), indicating its high durability (Figure S14 in the SI). Here, the photocatalytic O_2 evolution proceeds according to reaction paths (3)−(5).

$$\text{m-}Ag_2Mo_2O_7\text{-NW} + \text{vis} \rightarrow e^-\ (\text{CB}) + h^+\ (\text{VB}) \quad (3)$$

$$e^-\ (\text{CB}) + Ag^+ \rightarrow Ag \quad (4)$$

$$4h^+\ (\text{VB}) + 2H_2O \rightarrow O_2 + 4H^+ \quad (5)$$

CB and VB represent the conduction and valence bands of m-$Ag_2Mo_2O_7$-NW, respectively. A decrease in the activity for O_2 evolution in the course of the photocatalytic reaction is ascribed to the principle that metallic Ag formed by reduction of Ag^+ (eq 4) covers an active site for the reduction reaction and causes the light-shielding effect. Then we checked the excitation-wavelength dependence of the photocatalysis (Figure S15 in the SI). The onset wavelength of the activity for O_2 evolution agreed well with that of DRS. This clearly indicated that the O_2 evolution reaction proceeded by band-gap excitation of the $Ag_2Mo_2O_7$ nanowire and the photocatalytic reactions seen in Figure S11 in the SI are less likely to be affected by the plasmonic photocatalysis by the metallic Ag.[22] An apparent quantum yield (AQY) was determined to be 0.2% at 300 nm. To our best knowledge, this is the first example that the photocatalytic O_2 evolution reaction proceeds on $Ag_2Mo_2O_7$ regardless of the crystal systems and particle size. Besides, Gao et al. reported a pioneering work where a $Ba_2Mo_2O_7$ nanowire was hydrothermally synthesized using MoO_3, NaF, and $BaCl_2$; however, an addition of NaF to form HF into the reaction solution is vital to preparing the nanowire, indicating the different growth mechanism of the nanowire.[23]

In summary, we have demonstrated that the use of a commercially available MoO_3 particle as a starting material afforded the nanowire morphology of m-$Ag_2Mo_2O_7$. The nanowire possessed a highly crystalline nature and structural homogeneity, both of which were favorable to use as the photocatalyst. This facile approach provides new opportunities for engineering Ag−Mo−O materials working as visible-light-responsive photocatalysts for solar-to-fuel conversion.

■ ASSOCIATED CONTENT

Ⓢ Supporting Information

Experimental section, crystal structure, XRD patterns, FE-SEM, HR-TEM, elemental analyses, XPS, schematics, DRS, and photocatalytic O_2 evolution reaction. This material is available free of charge via the Internet at http://pubs.acs.org.

■ AUTHOR INFORMATION

Corresponding Author

*E-mail: ksaito@eng.niigata-u.ac.jp.

Notes

The authors declare no competing financial interest.

■ ACKNOWLEDGMENTS

This work was financially supported by PRESTO, The Kurata Memorial Hitachi Science and Technology Foundation.

■ REFERENCES

(1) Krol, R.; Liang, Y.; Schoonman, J. *J. Mater. Chem.* **2008**, *18*, 2311−2320.
(2) Yang, X.; Wolcott, A.; Wang, G.; Sobo, A.; Fitzmorris, R. C.; Qian, F.; Zhang, J. Z.; Li, Y. *Nano Lett.* **2009**, *9*, 2331−2336.
(3) Pendyala, C.; Jasinski, J. B.; Kim, J. H.; Vendra, V. K.; Lisenkov, S.; Menon, M.; Sunkara, M. *Small* **2012**, *4*, 6269−6275.
(4) Mayer, M. T.; Du, C.; Wang, D. *J. Am. Chem. Soc.* **2012**, *134*, 12406−12409.
(5) Oh, I.; Kye, J.; Hwang, S. *Nano Lett.* **2012**, *12*, 298−302.
(6) Liu, C.; Sun, J.; Tang, J.; Yang, P. *Nano Lett.* **2012**, *12*, 5407−5411.
(7) Goncalves, R.; Leite, L. D. T.; Leite, E. R. *ChemSusChem* **2012**, *5*, 2341−2347.
(8) Bao, N.; Shen, L.; Takata, T.; Lu, D.; Domen, K. *Chem. Lett.* **2006**, *35*, 318−319.
(9) Yu, J.; Kudo, A. *Adv. Funct. Mater.* **2006**, *16*, 2163−2169.
(10) Sun, J.; Liu, C.; Yang, P. *J. Am. Chem. Soc.* **2011**, *133*, 19306−19309.
(11) Saito, K.; Kudo, A. *Nanosci. Nanotechnol. Lett.* **2011**, *3*, 686−689.
(12) Wang, D.; Pierre, A.; Kibria, M. G.; Cui, K.; Han, X.; Bevan, K. H.; Guo, H.; Paradis, S.; Hakima, A.-R.; Mi, Z. *Nano Lett.* **2011**, *11*, 2353−2357.
(13) Feng, M.; Zhang, M.; Song, J.-M.; Li, X.-G.; Yu, S.-H. *ACS Nano* **2011**, *5*, 6726−6735.
(14) Yu, S.-H.; Liu, B.; Mo, M.-S.; Huang, J.-H.; Liu, X.-M.; Qian, Y.-T. *Adv. Funct. Mater.* **2003**, *13*, 639−647.
(15) Joshi, U. A.; Lee, J. S. *Small* **2005**, *1*, 1172−1176.
(16) Pacholski, C.; Kornowski, A.; Weller, H. *Angew. Chem., Int. Ed.* **2002**, *41*, 1188−1191.
(17) Penn, R. L. *J. Phys. Chem. B* **2004**, *108*, 12707−12712.
(18) Deng, Z.; Chen, D.; Tang, F.; Meng, X.; Ren, J.; Zhang, L. *J. Phys. Chem. C* **2007**, *111*, 5325−5330.
(19) Singh, D. P.; Sirota, B.; Talpatra, S.; Kohli, P.; Rebholz, C.; Aouadi, S. M. *J. Nanopart. Res.* **2012**, *14*, 781−792.
(20) Solodovnikova, Z. A.; Solodovnikova, S. F. *Acta Crystallogr., Sect. C* **2006**, *62*, i53−i56.
(21) Harriman, A.; Thomas, J. M.; Millward, G. R. *New J. Chem.* **1987**, *11*, 757−762.
(22) Zhu, Q.; Wang, W.-S.; Lin, L.; Gao, G.-Q.; Guo, H.-L.; Du, H.; Xu, A.-W. *J. Phys. Chem. C* **2013**, *117*, 5894−5900.
(23) Gao, P.; Xie, Y.; Ye, L.; Chen, Y.; Li, Z. *Chem. Lett.* **2006**, *35*, 162−163.